

Vertex-Linked ZnO₂S₂ Tetrahedra in the Oxysulfide BaZnOS: a New Coordination Environment for Zinc in a Condensed Solid

Sarah Broadley,[†] Zoltán A. Gál,[†] Furio Corà,[‡] Catherine F. Smura,[†] and Simon J. Clarke*[†]

Department of Chemistry, University of Oxford, Inorganic Chemistry Laboratory, South Parks Road, Oxford OX1 3QR, U.K., and Davy Faraday Research Laboratory, The Royal Institution of Great Britain, 21 Albemarle Street, London W1S 4BS, U.K.

Received July 25, 2005

The wide-band-gap semiconductor BaZnOS adopts a high-symmetry modification of the SrZnO₂ structure type and contains layers of vertex-linked ZnO₂S₂ tetrahedra, which represent a novel coordination environment for zinc in the solid state. BaZnOS: orthorhombic, space group *Cmcm*; $a = 3.9619(2)$ Å, $b = 12.8541(7)$ Å, $c = 6.1175(4)$ Å, $Z = 4$. Diffuse-reflectance spectroscopy measurements reveal a direct band gap of 3.9(3) eV, consistent with the white color and the results of band structure calculations. The band gap is larger than those observed in ZnO and ZnS, consistent with the more ionic nature of BaZnOS. Attempts to dope this compound electronically have so far not proved possible.

Introduction

Oxychalcogenides are an underexplored class of material compared with pure oxides and chalcogenides. Ternary oxysulfides (i.e., those containing the cation of one electro-positive element together with oxide and sulfide) are known for the elements of group 3, and the lanthanides and Ln₂O₂S compositions (Ln = lanthanide) are of interest for application in inorganic phosphor materials.¹ Apart from these compounds, the only ternaries that have been structurally characterized are ZrOS,^{2,3} HfOS,⁴ and the oxysulfides of the heavier pnictogens Bi₂O₂S⁵ and Sb₂OS₂.⁶ The different sizes and chemical requirements of the oxide ions and the ions of the heavier chalcogenides invariably mean that in oxychalcogenides the different anions are crystallographically ordered. In quaternary and higher oxychalcogenides in which one or more of the cations of electropositive elements are coordinated by both oxide and chalcogenide anions, oxide is often coordinated mainly by “hard” cations, while the more

polarizable chalcogenide ions are often coordinated mainly by “softer”, more polarizing cations. A range of layered structure types results. In the series LnCuOS, fluorite-type LnO layers alternate with antifluorite-type CuS layers, and in the quinary compounds A₂MO₂Cu₂S₂ (A = electropositive metal and M = transition metal), the same CuS layers intergrow with A₂MO₂ layers, which contain square MO₂ sheets (similar to the CuO₂ sheets in the cuprate superconductors). Both the LnCuOS series^{7,8} and Sr₂ZnO₂Cu₂S₂^{9–11} have been investigated as possible p-type transparent semiconductors because the top of the valence band is composed of Cu 3d/S 3p antibonding states and is relatively easily depleted.¹² We are investigating this series of layered oxychalcogenides, and while investigating the synthesis of the as-yet elusive target Ba₂ZnO₂Cu₂S₂, we synthesized the novel layered oxysulfide BaZnOS, which has a new structure type related to those of other ternary oxides and chalcogenides of alkaline earth and group 10 metals. This compound has a coordination environment for Zn, which has previously only been observed in molecular systems.

* To whom correspondence should be addressed. E-mail: simon.clarke@chem.ox.ac.uk. Tel: 44 1865 272600. Fax: 44 1865 272690.

[†] University of Oxford.

[‡] The Royal Institution of Great Britain.

- (1) Greskovich, C.; Duclos, S. *Annu. Rev. Mater. Sci.* **1997**, *27*, 69.
- (2) Gleizes, A.; Jeannin, Y. P.; Maire, N. *Bull. Soc. Chim. Fr.* **1974**, 1317.
- (3) Jellinek, F. *Acta Chem. Scand.* **1962**, *16*, 791.
- (4) Stocks, K.; Eulenberger, G.; Hahn, H. *Z. Anorg. Allg. Chem.* **1980**, *463*, 105.
- (5) Koyama, E.; Nakai, I.; Nagashima, K. *Acta Crystallogr. B* **1984**, *40*, 105.
- (6) Bonazzi, P.; Menchetti, S.; Sabelli, C. *Neues Jahrb. Mineral. Monatsh.* **1987**, 557.

- (7) Ueda, K.; Inoue, S.; Hirose, S.; Kawazoe, H.; Hosono, H. *Appl. Phys. Lett.* **2000**, *77*, 2701.
- (8) Hiramoto, H.; Kamioka, H.; Ueda, K.; Hirano, M.; Hosono, H. *J. Ceram. Soc. Jpn.* **2005**, *113*, 10.
- (9) Zhu, W. J.; Hor, P. H. *J. Solid State Chem.* **1997**, *130*, 319.
- (10) Hirose, H.; Ueda, K.; Kawazoe, H.; Hosono, H. *Chem. Mater.* **2002**, *14*, 1037.
- (11) Broadley, S.; Gál, Z. A.; Caldwell, H.; Smura, C. F.; Clarke, S. J., unpublished results.
- (12) Vajenine, G. V.; Hoffmann, R. *Inorg. Chem.* **1996**, *35*, 451.

Experimental Section

Synthesis. BaZnOS crystals used for the crystal structure analysis were formed in the reaction between BaS, ZnO (Alfa 99.9995%), and Cu₂O in the molar ratio 2:1:1 (in an attempt to synthesize Ba₂ZnO₂Cu₂S₂) at 920 °C for 24 h. The mixture was molten at this temperature, and it is presumed that the crystals grow in a copper sulfide-rich flux. Powder X-ray diffraction (PXRD) measurements showed that BaZnOS was the majority product from this reaction. Subsequently, pure BaZnOS powder, used for the other measurements, was made on the 2-g scale by reacting together equimolar quantities of BaS and ZnO at 920 °C for 24 h and was judged to be phase pure according to PXRD measurements. In both syntheses, the reagents were cold pressed into pellets and contained in alumina crucibles inside sealed, predried, evacuated silica tubes. BaS was made by reacting BaCO₃ (Alfa 99.95%) with CS₂ vapor (transported by bubbling argon through the liquid) at 900 °C for 12 h in a flow system. (**Caution!** CS₂ is highly toxic and highly flammable. The gas emerging from the flow system was passed through hydroxide bleach to destroy excess CS₂, and the flow system was purged with pure argon after the apparatus had cooled to room temperature; the entire apparatus was contained in a fume hood.) Cu₂O was made by reacting CuO (Aldrich 99.99%) with Cu powder (Alfa 99.999%) at 1000 °C in a sealed silica tube for 24 h. BaS and copper powder are air-sensitive, and manipulations of the solid reagents were performed in a Glovebox Technology argon-filled glovebox with an O₂ and H₂O content < 1 ppm. BaZnOS was found to be stable in air.

Structural Analysis. PXRD measurements were used for the analysis of the reagents and products prepared as described above. A Philips X'pert diffractometer equipped with an X'cellerator detector and with monochromatic Cu K α ₁ radiation selected using a Ge(111) monochromator was used. The structure of BaZnOS was determined from single-crystal XRD data collected using a Nonius Kappa CCD diffractometer using Mo K α radiation ($\lambda = 0.71073$ Å). The crystal was transparent and colorless with dimensions 0.04 × 0.02 × 0.01 mm³. Structure solution was carried out using Direct Methods via SHELXS-97,¹³ as implemented in the WinGX suite;¹⁴ absorption corrections were numerical based on face indexing.¹⁵ Full-matrix least-squares refinements on F^2 were carried out using SHELXL-97.¹³

Chemical Analysis. Quantitative elemental analysis on single crystals for barium, zinc, and sulfur was carried out on a JEOL JSM-840A scanning electron microscope equipped with an Oxford Instruments ISIS300 energy-dispersive X-ray analyzer. The ratios of the elements Zn/Ba/S were determined to be 1:1.1(1):1.0(1) by taking the average of several spot measurements made on the same crystal as that used in the single-crystal XRD study. This apparatus cannot be used for quantitative analysis of light atoms such as O.

X-ray Photoelectron Spectroscopy (XPS) Measurements. Valence-level spectra were recorded on a sintered pellet of material using the Scienta ESCA-300 spectrometer at the NCESS facility, Daresbury Laboratory, Cheshire, U.K. Ionization was performed using monochromatic Al K α radiation (1.4867 keV). All spectra were recorded using a pass energy of 150 eV and a takeoff angle of 90°. Sample charging was stabilized by a low-energy "flood gun" that irradiated the sample with electrons with a kinetic energy of 7 eV.

Diffuse-Reflectance Spectroscopy Measurements. Measurement was carried out at room temperature using a Varian Cary 500 UV–vis–near-IR spectrophotometer equipped with a double-beam photomultiplier tube and a lead sulfide detector. Reflectance measurement of the sample was made relative to poly(tetrafluoroethylene): the reference material was used to establish a baseline, and the absolute reflectivity of a sample was then calculated from that of the reference. Data were collected in the wavelength range 260–3000 nm. The Kubelka–Munk function¹⁶ was used to convert diffuse-reflectance data to absorbance spectra.

Band Structure Calculations. Electronic structure calculations employed the CRYSTAL code¹⁷ and the B3LYP hybrid exchange¹⁸ within density functional theory. The B3LYP functional was chosen because it has been shown to reproduce fairly well experimental values of the band gaps for a variety of materials,¹⁹ including ZnS.²⁰ We employed an all-electron basis set of triple valence plus polarization quality for Zn, O, and S and a small-core pseudopotential for Ba; the input file for CRYSTAL03 is given as Supporting Information.

Results and Discussion

Structure. Indexing of the single-crystal XRD pattern suggested a *C*-centered orthorhombic cell with $a = 3.9619(2)$ Å, $b = 12.8541(7)$ Å, and $c = 6.1175(4)$ Å. Three possible candidate space groups consistent with the observed systematic extinctions were initially identified: *Cmcm* (No. 63, centrosymmetric), *Cmc2*₁ (No. 36, non-centrosymmetric), and *C2cm* (No. 40, non-centrosymmetric). Because *E* statistics strongly favored a centrosymmetric structure, *Cmcm* was initially selected as a starting space group for structure determination. Both direct methods and Patterson methods produced initial starting models with reasonably low *R* values (below 20%); however, further refinement of these models resulted in chemically unrealistic distances and/or environments for atoms identified as Ba and Zn. Lowering the space group to either of the noncentrosymmetric choices provided equally uninterpretable results. Synthesized precession photographs of the $n = 0, 1,$ and 2 layers along each zone axis were carried out, but no signs of peak splitting due to either twinning or crystal damage were found. Reindexation of the observed intensities was carried out based on the primitive monoclinic cell ($a = 3.962$ Å, $b = 6.117$ Å, $c = 6.725$ Å, and $\beta = 107.13^\circ$), congruent with the original *C*-centered orthorhombic cell but with half of the cell volume. A structural model (with an initial *R* value below 5%) was obtained using direct methods in *P2*₁/*m*, and further refinements proceeded without any complications. Upon inspection, the presence of the further mirror planes required for orthorhombic symmetry was confirmed, and the atomic coordinates were transformed for the original orthorhombic cell. Refinements in *Cmcm* using this model gave satisfactory residuals, and we conclude that the structure does have

(16) Kubelka, P.; Munk, F. *Z. Tech. Phys.* **1931**, *12*, 593.

(17) Saunders, V. R.; Dovesi, R.; Roetti, C.; Orlando, R.; Zichovic-Wilson, C. M.; Harrison, N. M.; Doll, K.; Civalieri, B.; Bush, I. J.; D'Arco, Ph.; Llunell, M. *CRYSTAL03 User's Manual*; University of Torino: Torino, Italy, 2003.

(18) Becke, A. D. *J. Chem. Phys.* **1993**, *98*, 5648.

(19) Muscat, J.; Wander, A.; Harrison, N. M. *Chem. Phys. Lett.* **2001**, *342*, 397.

(20) Catti, M. *Phys. Rev. B* **2002**, *65*, 224115.

(13) Sheldrick, G. M. *SHELX97: Programs for Crystal Structure Analysis*, Release 97-2; University of Göttingen: Göttingen, Germany, 1997. <http://shelx.uni-ac.gwdg.de/SHELX/>.

(14) Farrugia, L. J. *J. Appl. Crystallogr.* **1999**, *32*, 837.

(15) Alcock, N. W. *Crystallogr. Comput.* **1970**, *271*.

Table 1. Results of Refinement of the Structure of BaZnOS against Single-Crystal XRD Data

formula	BaZnOS
radiation	Mo K α ($\lambda = 0.710\ 73\ \text{\AA}$)
instrument	Enraf Nonius Kappa FR590 CCD
physical form	colorless prism
T/K	240(2)
crystal system	orthorhombic
space group	<i>Cmcm</i> (No. 63)
formula weight	250.79
$a/\text{\AA}$	3.9619(2)
$b/\text{\AA}$	12.8541(7)
$c/\text{\AA}$	6.1175(4)
$V/\text{\AA}^3$	311.54(3)
Z	4
$\rho_{\text{calc}}/(\text{mg m}^{-3})$	5.346(1)
independent reflections	408
no. of variables	18
GOF on F^2	1.067
R1	0.0188
wR2	0.0364

Table 2. Structural Parameters for BaZnOS Obtained from Refinement against Single-Crystal XRD Data

atom	site	x	y	z	$U(\text{eq})^a/\text{\AA}^2$
Ba	4c	0	0.39205(2)	$1/4$	0.0091(1)
Zn	4c	0	0.09778(3)	$1/4$	0.0080(1)
S	4c	0	0.69394(8)	$1/4$	0.0092(2)
O	4a	0	0	0	0.0121(6)

^a $U(\text{eq})$ is defined as one-third of the orthogonalized U_{ij} tensor.

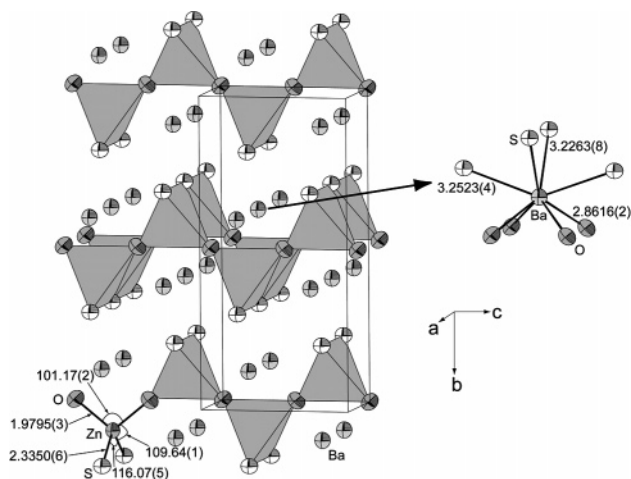
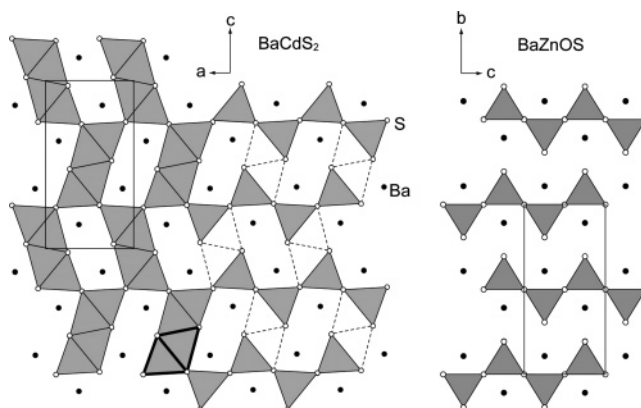
Table 3. Metal–Anion Bond Lengths and Selected Bond Angles for BaZnOS

	bond length/ \AA		bond angle/deg
Ba–O [4] ^a	2.8616(2)	O–Zn–O [1] ^a	101.17(2)
Ba–S [2] ^a	3.2263(8)	O–Zn–S [4] ^a	109.64(1)
Ba–S [2] ^a	3.2523(4)	S–Zn–S [1] ^a	116.07(5)
Zn–O [2] ^a	1.9795(3)		
Zn–S [2] ^a	2.3350(6)		

^a The numbers in square brackets indicate the number of bonds or angles of a particular type.

orthorhombic symmetry. The results are summarized in Table 1. As for the apparent failure of direct methods in the orthorhombic case (equally poor models were obtained by both SHELXS and SIR routines implemented within WinGX¹⁴), this may be a consequence of the fact that only the lightest (O) atom in the structure has a Wyckoff site fixed by symmetry (0, 0, 0) (4a), while the other, heavier atoms occupy more general (0, y , $1/4$) (4c) sites, where the y coordinate is free. This is not the case when working with the lower symmetry (monoclinic) cell. The refined atomic positions are listed in Table 2, and selected bond lengths and angles are listed in Table 3.

The structure of BaZnOS is shown in Figure 1. Zn atoms are in tetrahedral coordination by two oxygen atoms at 1.9795(3) \AA and two sulfur atoms at 2.3350(6) \AA . These distances are very similar to the distances in the binary compounds in which Zn is also in tetrahedral coordination. (ZnO: 3 \times O at 1.9754 \AA , 1 \times O at 1.9833 \AA .²¹ ZnS: wurtzite, 3 \times S at 2.3343 \AA , 1 \times S at 2.3378 \AA ; sphalerite,

**Figure 1.** Crystal structure of BaZnOS showing the ZnO₂S₂ tetrahedra and with the coordination environment of barium shown as the inset. Unique bond lengths and angles are given in angstroms and degrees. Displacement ellipsoids are shown at the 99.9% level.**Figure 2.** Structure of BaCdS₂³³ (left) compared with a comparable view of BaZnOS (right). The right-hand part of the representation of BaCdS₂ shows how the layers of corner-linked tetrahedra in BaZnOS pucker in forming the related SrZnO₂³¹ structure. The dotted lines on this part of the figure show how the three-dimensional framework of edge- and corner-linked trigonal bipyramids (one of these is emphasized in bold) in the BaCdS₂ structure is assembled.

4 \times S at 2.3456 \AA .²²) The ZnO₂S₂ tetrahedra share all of their vertices and form two sets of parallel chains along the a and c axes. The puckered zinc oxysulfide layers formed by the joining of these chains are separated by barium cations in eight-coordination [4 \times O at 2.8616(2) \AA , 2 \times S at 3.2263(8) \AA , and 2 \times S at 3.2523(4) \AA]. The barium coordination environment is a distorted biaugmented triangular prism: the two larger rectangular faces of a BaO₄S₂ isosceles triangular prism are capped by the remaining two S atoms. Bond valence sum calculations carried out using the EUTAX package²³ produced bond valence sums as follows: Ba, 2.029; Zn, 1.981; S, 2.207; O, 1.803 (consistent with the expected values).

Few zinc-containing oxysulfides have been reported previously. The naturally occurring mineral genthelvite²⁴ [Zn₈(Be₆Si₆O₂₄)S₂] has the sodalite-type structure, and zinc is in tetrahedral coordination by three framework oxygen atoms

(21) Sawada, H.; Wang, R.; Sleight, A. W. *J. Solid State Chem.* **1996**, 122, 148.

(22) Xu, Y.-N.; Ching, W. Y. *Phys. Rev. B* **1993**, 48, 4335. Rabadanov, M. Kh.; Loshmanov, A. A.; Shaldin, Yu. V. *Kristallografiya* **1997**, 42, 649.

(23) Brese, N. E.; O'Keeffe, M. *Acta Crystallogr., Sect. B* **1991**, 47, 192.

(24) Hassan, I.; Grundy, H. D. *Am. Miner.* **1985**, 70, 186.

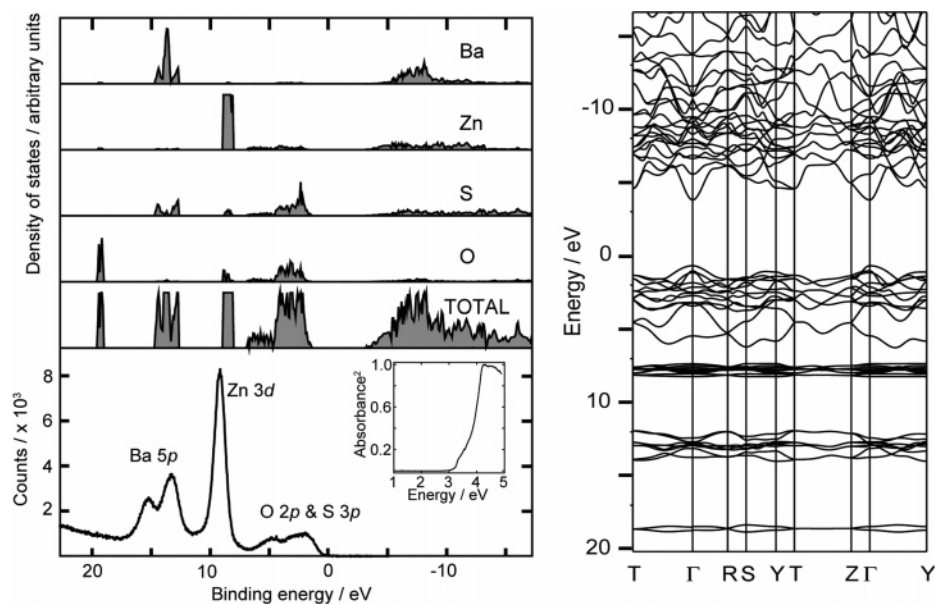


Figure 3. Calculated band structure (right) and calculated DOSs for BaZnOS compared with the measured XPS spectrum in the valence region (left). The energy scale of the calculations has been shifted to correspond to the scale used for the experimentally determined binding energies. The inset shows the result of the diffuse-reflectance spectroscopy measurement.

and the sulfide inside the β cage. The cadmium analogue is isostructural.²⁵ In the akermanite analogues $\text{La}_2\text{ZnGa}_2\text{S}_6\text{O}$, $\text{Sr}_2\text{ZnGe}_2\text{S}_6\text{O}$, and $\text{Ba}_2\text{ZnGe}_2\text{S}_6\text{O}$,²⁶ zinc is in tetrahedral coordination by sulfide only. CaZnOS has been reported²⁷ in which zinc and sulfur form hexagonal puckered ZnS layers with Zn–S bonds of 2.3673 Å and zinc is further coordinated by one O atom at 1.9240 Å. Ca is in six-coordination ($3 \times \text{O}$ and $3 \times \text{S}$) in CaZnOS , so this structure is quite different from that of BaZnOS . We are unaware of any condensed phases containing ZnO_2S_2 tetrahedra, although such a coordination environment for zinc has been reported in the molecular species $[\text{Zn}(\text{C}_2\text{H}_3\text{O}_2)_2(\text{C}_4\text{H}_8\text{N}_2\text{S}_2)] \cdot \text{H}_2\text{O}$ ²⁸ and $[\text{Zn}(\text{OEtCOCH}=\text{CSCH}_3)_2]$ ²⁹ and the bimetallic examples $[\text{Zn}\{\mu\text{-SSi}(\text{O}i\text{Bu})_3\}(\text{acac})_2]$ and $\{(\text{Bu}i\text{O})_3\text{Si}\}(\text{H}_2\text{O})_2\text{Zn}\{\mu\text{-SSi}(\text{O}i\text{Bu})_3\}\text{Zn}(\text{acac})\{\text{SSi}(\text{O}i\text{Bu})_3\}\}$.³⁰ The only other reported zinc-containing oxsulfide, $\text{Sr}_2\text{ZnO}_2\text{Cu}_2\text{S}_2$, contains zinc in pseudo-octahedral coordination by four equatorial oxygen atoms at 2.006 Å and two weakly coordinating axial sulfur atoms at 3.051 Å.⁹ We have not yet been successful in synthesizing the strontium analogue SrZnOS .

SrZnO_2 ³¹ and BaMnS_2 ³² are structurally similar to BaZnOS and have ZnO_2 and MnS_2 layers similar to the ZnOS layers described here. However, these compounds are distorted, with the alkaline-earth cations in seven- rather than eight-coordination and with puckered ZnO_2 and MnS_2 layers.

BaCdS_2 ³³ and BaCdO_2 ³⁴ also have related structures: the barium cations are in seven-coordination as in SrZnO_2 , and the larger Cd^{2+} cations are in five-coordinate sites, which result from the capping of each tetrahedron in the SrZnO_2 -type structure by one of the vertexes of a tetrahedron in a neighboring layer. The result is a three-dimensional CdO_2 or CdS_2 framework composed of edge- and vertex-sharing CdO_5 or CdS_5 distorted trigonal bipyramids. The relationship between these structures is shown in Figure 2. The topology of the ZnOS layers in BaZnOS is also related to the extremely puckered CuS_2 layers in wolfsbergite SbCuS_2 .³⁵

Electronic Structure. Measurement of the absorption spectrum of BaZnOS powder using diffuse-reflectance spectroscopy revealed a dominant absorption that is assigned to a room-temperature direct band gap of 3.9(3) eV. Lower energy transitions were observed in the spectrum and are presumed to arise from impurities (they are much more intense than absorptions that would arise from indirect transitions). This band gap is somewhat larger than the room-temperature values of 3.3 and 3.67 eV for wurtzite ZnO ³⁶ and sphalerite ZnS ,³⁷ respectively. Bands for BaZnOS were calculated at the geometry-optimized crystal structure, characterized by lattice parameters $a = 4.0312$ Å, $b = 13.1026$ Å, and $c = 6.2101$ Å, which are each about 2% larger than the experimentally determined lattice parameters; in this optimized structure, the Zn–O and Zn–S bond distances of 1.983 and 2.384 Å, respectively, are overestimated by 0.2% and 2%, respectively, relative to the experimentally determined values. Overestimation of this

(25) Dann, S. E.; Weller, M. T. *Inorg. Chem.* **1996**, *35*, 555.

(26) Teske, C. L. *Z. Anorg. Allg. Chem.* **1985**, *531*, 52. Teske, C. L. *Z. Naturforsch. B* **1980**, *35*, 672.

(27) Petrova, S. A.; Mar'evich, V. P.; Zakharov, R. G.; Selivanov, E. N.; Chumarev, V. M.; Udoveva, L. Yu. *Dokl. Akad. Nauk* **2003**, *393*, 52.

(28) Razak, I. A.; Usman, A.; Fun, H. K.; Yamin, B. M.; Bohari, M.; Keat, G. W. *Acta Crystallogr., Sect. C* **2002**, *58*, m31.

(29) Hoskins, B. F.; Pannan, C. D. *Inorg. Nucl. Chem. Lett.* **1975**, *11*, 405.

(30) Becker, B.; Dolega, A.; Konitz, A.; Wojnowski, W. *Polyhedron* **2001**, *20*, 949.

(31) von Schnering, H. G.; Hoppe, R. *Z. Anorg. Allg. Chem.* **1961**, *312*, 87.

(32) Schmitz, D.; Bronger, W. *Z. Anorg. Allg. Chem.* **1973**, *402*, 225.

(33) Iglesias, J. E.; Pachali, K. E.; Steinfink, H. J. *Solid State Chem.* **1974**, *9*, 6.

(34) von Schnering, H. G. *Z. Anorg. Allg. Chem.* **1962**, *314*, 144.

(35) Hofmann, W. *Fortschr. Mineral.* **1932**, *17*, 422.

(36) Mang, A.; Reimann, K.; Rübenacke, S. *Solid State Commun.* **1995**, *94*, 251.

(37) Ves, S.; Schwarz, U.; Christensen, N. E.; Syassen, K.; Cardona, M. *Phys. Rev. B* **1990**, *42*, 9113.

order is typical of the B3LYP functional [5].³⁸ Calculations on the optimized structure indicate a direct 0 K band gap in the Γ point of reciprocal space of 4.5 eV. This value is somewhat larger than the room-temperature experimentally determined value of 3.9(3) eV, but it is in line with the calculation of the band gap of 3.9 eV for ZnS, which was carried out using the same settings and which also overestimates the band gap (experimental band gap for ZnS is 3.67 eV). The calculated band structure and density of states (DOSs; total and projected onto the atomic basis sets) are shown in Figure 3, where the valence-band XPS spectrum is also shown for comparison. The projected DOSs confirm the assignment of the experimental signals, in order of decreasing binding energies, to the Ba 5p (14 eV), Zn 3d (9.2 eV), and O 2p/S 3p levels (3 eV), respectively. The valence band extends for approximately 6 eV and is composed mainly of overlapping O 2p and S 3p states; the O 2p state dominates the lower part of the valence band, while the top of the valence band has predominantly S 3p character. The bottom of the conduction band is dominated by a highly dispersive Zn 4s band; the fundamental gap therefore corresponds to a transition between S 3p and Zn 4s levels. Ba 6s/p states are approximately 2 eV above the bottom of the conduction band. Attempts to electron dope this material, by heating the powder in zinc vapor at 1000 °C in a sealed silica tube, were unsuccessful. Other attempts at electron or hole doping are in progress. Investigations of structurally related oxychalcogenides with magnetic ions on

the tetrahedral sites that would invite comparison with the antiferromagnet BaMnS₂^{32,39} are also in progress.

Conclusions. BaZnOS is the first example of an extended solid containing zinc in the tetrahedral ZnO₂S₂ environment, and the structure is a higher symmetry analogue of the structures adopted by SrZnO₂, BaMnS₂, BaCdO₂, and BaCdS₂. Measurements and calculations of the electronic structure show a band gap of 3.9(3) eV, larger than the corresponding values in ZnS and ZnO and consistent with the more ionic nature of BaZnOS.

Acknowledgment. We thank Dr. D. S.-L. Law for assistance with the XPS measurements and EPSRC for access to this facility. We thank Professor P. S. Halasyamani and Dr. Kang Min Ok (Department of Chemistry, University of Houston, Houston, TX) for performing the diffuse-reflectance spectroscopy measurements and Dr. N. Charnley (Department of Earth Sciences, University of Oxford, Oxford, U.K.) for access to the EDX facility. F.C. acknowledges the support of an EPSRC Advanced Fellowship.

Note Added in Proof. One reviewer suggested that the apparent failure of direct methods in the space group *Cmcm* may be related to the fact that the atomic numbers of the elements in the compound approximately form a geometric progression.

Supporting Information Available: A crystallographic information file (CIF) and the CRYSTAL03 input file corresponding to the optimized geometry including all of the computational parameters are available. This material is available free of charge via the Internet at <http://pubs.acs.org>.

IC0512400

(38) Corà, F.; Alfredsson, M.; Mallia, G.; Middlemiss, D. S.; Mackrodt, W. C.; Dovesi, R.; Orlando, R. In *Principles and Applications of Density Functional Theory in Inorganic Chemistry*; Kaltsoyannis, N., McGrady, J. E., Eds.; Structure and Bonding 113; Springer-Verlag: Heidelberg, Germany, 2004; pp 171–232.

(39) Gonen, Z. S.; Fettinger, J. C.; Eichhorn, B. *J. Solid State Chem.* **2000**, *155*, 305.